

DSCC2015-9899

**SPRING-MASS WALKING WITH ATRIAS IN 3D:
ROBUST GAIT CONTROL SPANNING ZERO TO 4.3 KPH
ON A HEAVILY UNDERACTUATED BIPEDAL ROBOT**

Siavash Rezazadeh
rezazads@onid.orst.edu

Christian Hubicki
hubickic@onid.orst.edu

Mikhail Jones
jonesmik@onid.orst.edu

Andrew Peekema
peekemaa@onid.orst.edu

Johnathan Van Why
vanwhyj@onid.orst.edu

Andy Abate
abatea@onid.orst.edu

Jonathan Hurst
jonathan.hurst@oregonstate.edu

Dynamic Robotics Laboratory, School of Mechanical, Industrial and Manufacturing Engineering
Oregon State University, Corvallis, Oregon 97331

ABSTRACT

We present a reduced-order approach for robust, dynamic, and efficient bipedal locomotion control, culminating in 3D balancing and walking with ATRIAS, a heavily underactuated legged robot. These results are a development toward solving a number of enduring challenges in bipedal locomotion: achieving robust 3D gaits at various speeds and transitioning between them, all while minimally draining on-board energy supplies. Our reduced-order control methodology works by extracting and exploiting general dynamical behaviors from the spring-mass model of bipedal walking. When implemented on a robot with spring-mass passive dynamics, e.g. ATRIAS, this controller is sufficiently robust to balance while subjected to pushes, kicks, and successive dodgeball strikes. The controller further allowed smooth transitions between stepping in place and walking at a variety of speeds (up to 1.2 m/s). The resulting gait dynamics also match qualitatively to the reduced-order model, and additionally, measurements of human walking. We argue that the presented locomotion performance is compelling evidence of the effectiveness of the presented approach; both the control concepts and the practice of building robots with passive dynamics

to accommodate them.

INTRODUCTION

We present 3D bipedal walking control for the dynamic bipedal robot, ATRIAS (Fig. 1), by building controllers on a foundation of insights from a reduced-order “spring-mass” math model. This work is aimed at tackling an enduring set of challenges in bipedal robotics: fast 3D locomotion that is efficient and robust to disturbances. Further, we want the ability to transition between gaits of different speeds, including slowing to and starting from zero velocity. This set of demands is challenging from a generalized formal control approach because of various inconvenient mathematical properties; legged systems are typically cast as nonlinear, hybrid-dynamical, and nonholonomic systems, which at the same time, because of the very nature of walking, require highly robust control algorithms.

Bipedal robots are also increasingly becoming underactuated, i.e. a system with fewer actuators than degrees of freedom [1]. Underactuation is problematic for nonlinear control methods; as degrees of underactuation increase, handy techniques like feedback-linearization decline in the scope of their utility.

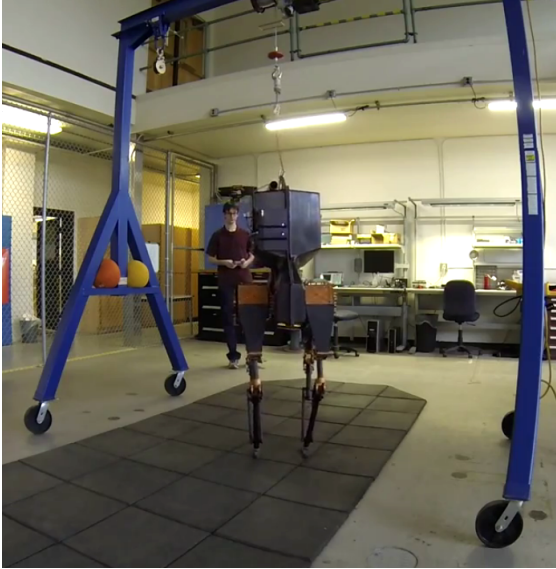


FIGURE 1: ATRIAS, A HUMAN-SCALE BIPEDAL “SPRING-MASS” ROBOT DESIGNED TO WALK AND RUN IN THREE DIMENSIONS.

Whenever a robot does not have an actuated foot planted on rigid ground, it is effectively underactuated. As a result, the faster legged robots move and the rougher the terrain they encounter, it becomes increasingly impractical to avoid these underactuated domains. Further, there are compelling reasons, both mechanical and dynamical, for removing actuators from certain degrees of freedom (see more in the robot design section).

With these facts in mind, our robotic platform is built to embody an underactuated and compliant “spring-mass” model (Fig. 2A), and our control reckons with the severe underactuation that results. ATRIAS has twelve degrees of freedom when walking, but just six actuators. However, by numerically analyzing the spring-mass model, we identify important targets and structures of control that can be regulated on the full-order robot which approximates it.

We organize the remainder of this paper as follows. We begin by surveying existing control methods for 3D, underactuated, and spring-mass locomotion. 2) The design philosophy of our spring-mass robot, ATRIAS, and its implementation are briefly described. 3) We then build a controller incrementally from a 1D idealized model, to a 3D model, to the full 12-degree-of-freedom robot. 4) We show that this controller can regulate speeds ranging from 0 m/s to 1.2 m/s and transition between them. 5) With a set of perturbation experiments, we demonstrate the robustness of the controller and 6) argue in our conclusions for the thoughtful cooperation between the tasks of robot design and control.

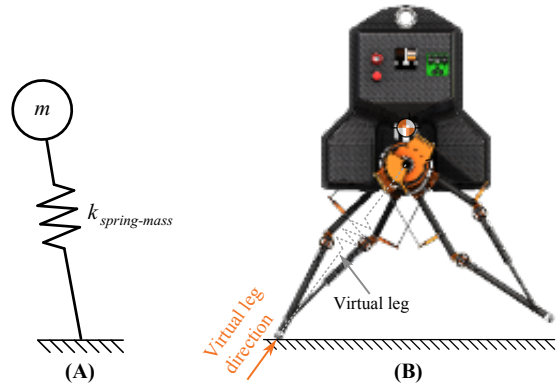


FIGURE 2: THE DESIGN PHILOSOPHY OF ATRIAS, WHICH MAXIMALLY EMBODIES THE “SPRING-MASS” MODEL OF WALKING AND RUNNING. A) THE SPRING MASS MODEL WITH A POINT MASS BODY AND MASS-LESS LEG SPRING. B) ATRIAS WITH A VIRTUAL LEG SPRING OVERLAID.

Existing Methods

This work primarily concerns three categories of legged robot control: bipedal robots that are 1) controlled in 3D, 2) controlled while underactuated, 3) are controlled via spring-mass insights, and combinations thereof.

The Raibert hoppers were among the earliest actuated legged machines to maneuver in three dimensions [2]. These robots hopped around, powered by a air-hose tether, and stabilized with a degree of agility that is still impressive to this day. More than a decade later, Honda introduced ASIMO [3], a fully self-contained humanoid robot capable of walking (and now running) untethered by leveraging zero moment point methods [4]. More recently, researchers have incorporated better disturbance rejection into robotic bipeds by rapidly computing recovery maneuvers after a push [5, 6], and even extended it to systems with compliance [7]. One of the goals of this study is to imbue ATRIAS with the effective robustness of these push-recovery methods while being a fast and efficient walker.

Counterintuitively, one way to improve maneuverability and efficiency is to strategically *remove* actuators from a robot; i.e. deliberately rendering the system underactuated. Tad McGeer demonstrated this concept elegantly with passive-dynamic walkers [8]. These walkers had no actuators or control of any sort, and yet could gracefully walk using only a shallow slope as an energy source. In fact, the genesis of formal underactuated control methods temporally coincides with the popularity of the passive walking [9]. Later robots leveraged this philosophy of only including minimal actuators to make impressively efficient, but highly specialized, underactuated walking machines [10, 11].

This enthusiasm for underactuated control methods gave rise to hybrid zero dynamics (HZD) approaches [12]. HZD was used to make a number of robots walk in planar scenarios, including

MABEL [13] and AMBER [14] (MABEL was able to run when attached to its rotating boom [15]). These methods can theoretically extend to 3D locomotion [16], and experimental validation is currently in progress [17]. Other methods such as transverse linearization [18] and Differential Dynamic Programming [19] have shown promise in simple testbed robots and simulators. However, these underactuated methods are, by and large, trying to solve the grander general problem of underactuated control. Such approaches, although valuable, are extremely dependent on the accuracy of the model which makes them problematic for robust performance. As well, they are usually designed around a specific periodic orbit and transitioning among different orbits is a totally nontrivial task. For these reasons, we target our methods specifically at bipedal locomotion, and particularly, what is called *spring-mass* locomotion.

The spring-mass model, a simple point mass attached to a massless leg spring (Fig. 2A), was originally proposed as a math model for running in animals [20]. It's an alluring robot model partly because of its theoretically low energy cost. When this springy model bounces on the ground, the ground-reaction forces (i.e. the center-of-mass dynamics) yield a strong correlation to those of running humans. Later work in biology showed this model is applicable to running in a broad array of animals from cockroaches to ghost crabs [21]. These indications of biological relevance inspired researchers to control testbed running robots with spring-mass models in mind [22, 23]. More recent research has shown that the spring-mass model can also reproduce the walking dynamics of humans [24].

We aim to demonstrate this “human-like” spring-mass walking with ATRIAS in 3D at varied speeds. However, achieving this goal is more than just a matter of control. It requires that the robot is physically capable of exhibiting spring-mass dynamics, which is a function of mechanical design.

ROBOT DESIGN

Here we briefly describe the design philosophy and hardware implementation of the bipedal robot ATRIAS.

Design Philosophy

ATRIAS (Assume The Robot Is A Sphere [25]) is designed explicitly to maximally embody the spring-mass model, while including all the actuation and accoutrements necessary to walk (and ultimately run) untethered in three dimensions. As such, the robot's mechanical features are designed to approximate the spring-mass model's massless leg spring, a lumped body mass, and a pin-jointed toe contact.

The robot's legs are designed as lightweight carbon-fiber fourbar mechanisms to approximate the massless leg spring of the spring-mass model. Each leg uses two motors to swing the leg through a wide range of motion in the sagittal plane (Fig.

3A). Each leg also has a third abduction motor allow maneuverability in the frontal plane (Fig. 3B). Figure 3C illustrates how this leg mechanism extends and crouches.

Springs are critical for ATRIAS to replicate spring-mass model dynamics. Two large plate springs are placed in series between the leg mechanism and the motors. When force is applied to the leg, the springs deflect as illustrated in Fig. 3D. These springs have particularly low stiffness, which allows them to store significant gait energy. This cycling of energy between the gait and spring helps save gait energy that would otherwise be lost when its feet impact the ground. This is beneficial to the overall energy economy of the robot, which preliminarily reported a cost of transport of 1.0, less than a third the estimated energy cost of ASIMO [25].

To allow the foot to act as a pin joint, we simply constructed it as a pin joint. This tiny foot, best seen in Fig. 1, has no motors. A simple elastic cord connecting the foot and leg allows the the foot to impact the ground, permits the foot angle to mold to the ground geometry, and resets the foot back to a neutral position when unloaded. The force applied by the elastic cord is sufficiently small that it does not have a noticeable effect on the gait dynamics.

Hardware Details

ATRIAS' torso is equipped with a number of components that allow it to function completely off-tether. We use four 22.2V lithium-polymer batteries to supply on-board power (two in series, two in parallel). To measure orientation and angular velocity in the world frame, we installed an inertial measurement unit with a fiberoptic gyro. This and the remaining robot state information is read and reported to an onboard control computer 1000 times a second. The control computer receives simple commands, such as commanded velocity, from a remote GUI connected via a wireless bridge.

CONTROLLER DESIGN

In this section, the controller design and the corresponding stabilizing methods are presented and discussed. The approach presented here, in essence, is similar to our previous controller for 2D walking, which was based on step by step synthesis of a stable gait [26]. In 3D the underactuation problem becomes more prominent and thus the steps towards control of the full robot have to be taken more carefully. In this way, we start by presenting a new stabilizing controller for a 1D in-place spring-mass walker, stabilize in 3D, replace the lumped mass with a rigid body as the torso, and finally extend it for walking with nonzero velocity.

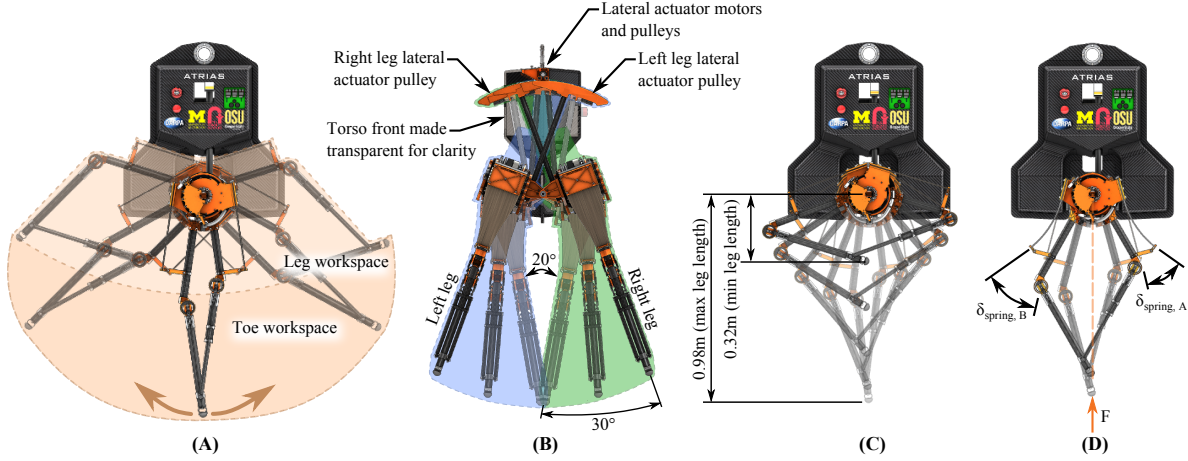


FIGURE 3: ATRIAS' DEGREES OF MECHANICAL FREEDOM AND RANGE OF MOTION [25]. **A)** THE FULL RANGE OF SAGITTAL LEG SWING. **B)** RANGE OF HIP ABDUCTION AND ADDUCTION. **C)** LEG EXTENSION AND CROUCHING CAPACITY **D)** MAXIMUM SPRING DEFLECTION.

One-Dimensional In-Place Walking

As the first step of our step-by-step control design, we start with the simplest case, i.e. a mass “walking” in a 1-D space (vertical axis) by alternating between two springy legs with damping (Fig. 4A). Note that this system is different from the vertical hopper first proposed and developed by Raibert [2] in which stable hopping was achieved by a feedforward impulsive fixed thrust during stance. For two different reasons, we seek another approach for stabilization of the in-place walking of this system. The first reason is that although Raibert’s energy injection scheme was well-suited for the fast pneumatic actuators of his hoppers (making impulsive energy injection feasible, which was shown by Koditschek and Buehler to have a stabilizing effect [27]), electrical actuators, due to their typically high inertias, cannot accommodate this. Furthermore, since the considered system has two legs, another variable, namely the phase between the two legs, exists which, as we will show, can be utilized for the stabilization purpose. This has the advantage of reserving the energy-injection scheme for other purposes (for walking forward, as it will be discussed later). To use this variable, we define periodic time-based trajectories for the neutral lengths of the springs (equivalent to the actuator positions in a series actuator-spring configuration), given by:

$$l_{m,1}(t) = \begin{cases} l_0 + l_{ret} \sin \omega t & \sin \omega t < 0 \\ l_0 & \sin \omega t \geq 0 \end{cases} \quad (1)$$

and

$$l_{m,2}(t) = \begin{cases} l_0 - l_{ret} \sin \omega t & \sin \omega t > 0 \\ l_0 & \sin \omega t \leq 0 \end{cases} \quad (2)$$

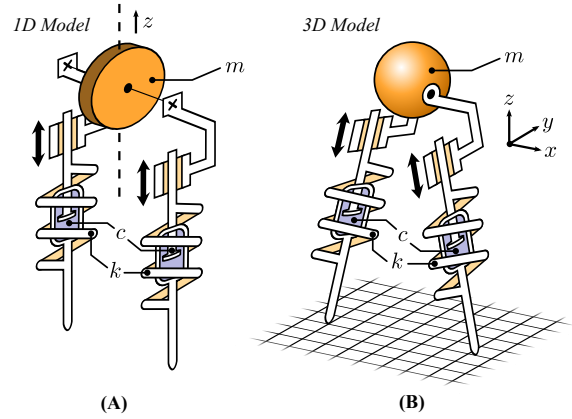


FIGURE 4: REDUCED-ORDER MODELS USED IN NUMERICAL INVESTIGATIONS. **(A)** A ONE-DIMENSIONAL (VERTICAL) SPRING-MASS MODEL WITH PRISMATIC ACTUATION AND LINEAR DISSIPATION AND **(B)** ITS EXTENSION TO THREE DIMENSIONS.

where ω and l_{ret} are preset values for frequency and retraction length, respectively. Intuitively, these time-based functions are two sinusoids with a phase difference of π/ω . They are clipped in their positive half-plane to only permit retraction (leg swing). In the stance phase they keep a fixed neutral length of l_0 (i.e. no energy injection). With these variables as control inputs, the dynamics of this system can be written as follows:

$$m\ddot{z} = F_1(z,t) + F_2(z,t) - mg \quad (3)$$

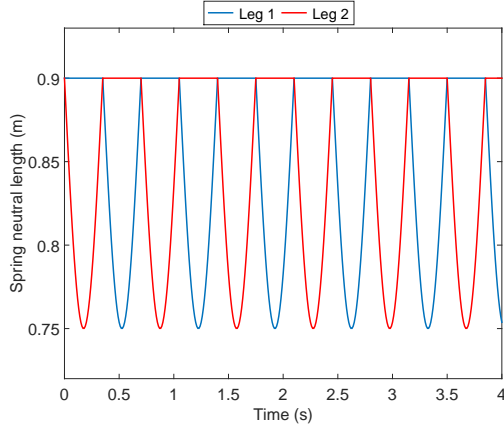


FIGURE 5: TIME-BASED FEEDFORWARD TRAJECTORIES OF NEUTRAL LENGTHS OF THE SPRINGS WHICH IS SHOWN TO HAVE A STABILIZING EFFECT.

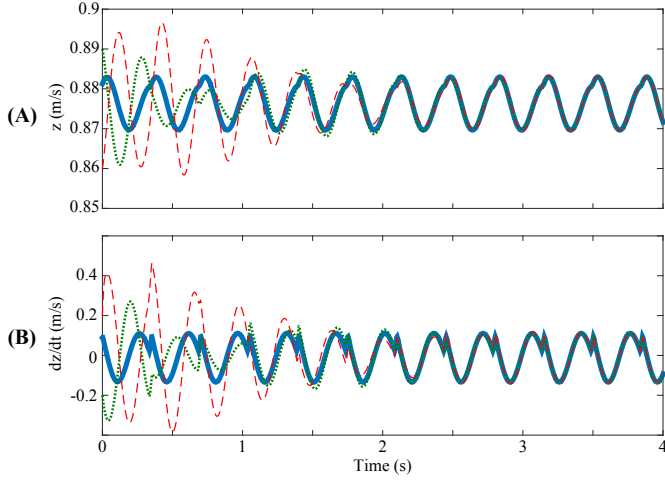


FIGURE 6: SIMULATION RESULTS OF THE ONE-DIMENSIONAL MODEL; THE SYSTEM IS GLOBALLY STABLE, AS FROM ANY INITIAL CONDITION IT WILL RETURN TO THE LIMIT CYCLE.

where

$$F_i(z, t) = \begin{cases} b(\dot{l}_{m,i} - \dot{z}) + k(l_{m,i} - z) & l_{m,i} > z \\ 0 & l_{m,i} \leq z \end{cases} \quad (4)$$

in which $i = 1, 2$ is the leg index. The stabilizing effect of time-based trajectories is not new. Specifically for spring-mass systems, Schmitt and Clark proposed a stabilizing time-based set of trajectories for stance phase energy injection [28]. However, as mentioned before, our method is different in that no stance phase control is performed and stabilization is achieved solely by the phase difference between the two legs. This has two ad-

vantages: 1) there is no requirement for sensing the start and end of stance phase (which is usually difficult and unreliable); and 2) the stance phase control can be reserved for other purposes, as we will discuss in the next sections.

Intuitively, the stability of the proposed system is achieved by taking advantage of the correlation between the height and the energy. In other words, if the energy is less than nominal, the height decreases, the swing leg hits the ground sooner, and starts injecting energy by continuing its extension, and vice versa. From another perspective, note that the set of dynamics shown in Eqns. (1)-(4) to a great extent resembles forced oscillations of a mass-spring-damper system, which always, after a transient due to initial conditions, approaches a stable trajectory. Although due to the unidirectionality of the leg forces the system is somewhat different here, simulations prove that the time-based control is indeed a stabilizing scheme. An example of such simulations is depicted in Figs. 5 (the feedforward trajectories) and 6, wherein from two different initial conditions the states approach the stable limit cycle (note that since the system is time-variant, rather than a phase plane plot, the states in terms of time have been presented). The parameters used approximately match those of ATRIAS: $k = 25000$ N/m, $b = 150$ Ns/m, and $m = 62$ kg. Also: $\omega = 2\pi/0.7$ rad/s, $l_0 = 0.9$ m, and $l_{ret} = 0.15$ m.

Having this stable control scheme for motion in a 1-D space, in the next section we present a horizontal-plane stabilization method for extension of the in-place walking to a 3-D space.

3D Stabilization of In-Place Walking

To design our horizontal plane control policy, we extend the 1D reduced order model of the previous section to 3D (Fig. 4B). The essential idea for controlling horizontal plane translational degrees of freedom is to use foot placement (location of the foot on the ground with respect to the mass) as a tool to apply a resistance for regulating the linear momentum in these directions to zero. For this purpose, a parameter sweep was performed, computing leg placements for a range of gait speeds and lateral touchdown velocities. These leg placements were chosen to enforce constraints on the mid-stance state of the model. This is an extension of an analysis performed by Raibert for velocity control of a planar hopper, [2] differing in that it focuses on lateral control for a 3D biped rather than planar velocity control with symmetrical stance phases. The reduced-order model consists of a point mass atop a spring model with lengthwise dynamics that match ATRIAS' lengthwise leg dynamics. A Boundary Value Problem (BVP) was formulated in which the lateral touchdown velocity was fixed, and several conditions (including gait velocity) were enforced at mid-stance. This BVP was solved using a collocation method for varying lateral touchdown velocities and gait velocities. The results of the parameter sweep are shown in Fig. 7. The lateral leg angle at touchdown which achieves the mid-stance conditions varies roughly linearly as a function

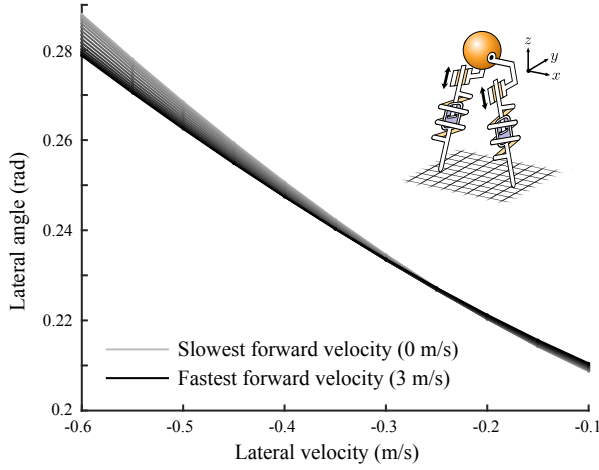


FIGURE 7: SIMULATION RESULTS OF THE ONE-DIMENSIONAL MODEL IN 3D; THE RELATIONSHIP BETWEEN THE STABILIZING LATERAL ANGLE AND THE VELOCITY IS ALMOST LINEAR.

of lateral velocity at touchdown. Additionally, the lateral angle does not vary significantly with forward velocity, even for velocities of 3 m/s, indicating that swing-phase lateral control for foot placement may be decoupled from the sagittal plane motion. Motivated by this study and due to these observations, we have chosen a lateral leg placement strategy that is linear in the lateral velocity and invariant to the forward velocity of the system. Specifically, we use a discrete PID for determination of the position of the feet in the horizontal plane:

$$\zeta_f = K_P \dot{\zeta} + K_D (\dot{\zeta} - \dot{\zeta}_{n-1}) + K_I \zeta \quad (5)$$

where $\zeta_{2 \times 1} = [x \ y]^T$ contains the horizontal plane coordinate variables, and K_P , K_D , and K_I are positive constants.

This discrete PID, together with the time-based trajectories proposed in the previous section stabilize the three translational degrees of freedom of the torso. In the next section we extend the controller for stabilization of the rotational degrees of freedom of the torso.

Control of Rotational Degrees of Freedom

For the representation of rotational degrees of freedom we adopt the standard yaw-roll-pitch convention. As mentioned previously, due to usage of two-point-contact feet and assuming that no slippage occurs, the yaw degree of freedom can be considered to be fixed. Therefore, roll and pitch are the two degrees of freedom to be controlled. The controller proposed in the previous sections for the translational degrees of freedom utilizes four actuators: two for time-based trajectories and two for horizontal plane foot placement of the swing leg. The two remaining ac-

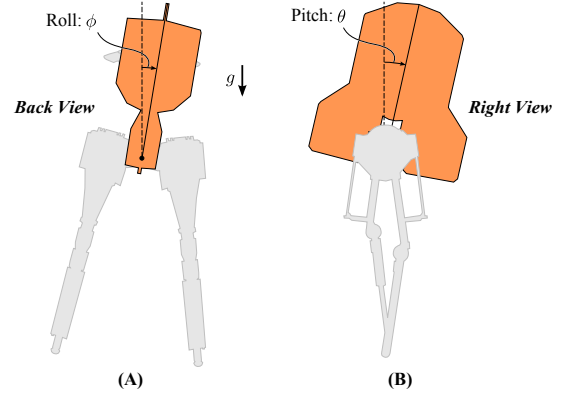


FIGURE 8: SCHEMATIC SHOWING DEFINITIONS OF TORSO ROTATION: (A) TORSO ROLL SHOWN FROM THE BACK VIEW AND (B) TORSO PITCH SHOWN FROM THE RIGHT VIEW.

tuators (of the stance leg) are used for controlling the rotational degrees of freedom.

As the first step for this purpose, we extend the reduced order model of the previous sections to have a torso with the two mentioned rotational degrees of freedom (Fig. 8). The dynamic equations can be written as:

$$D_{rom} \ddot{q}_{rom} + P_{rom}(q_{rom}, \dot{q}_{rom}) = f(q_{rom}, t) + B_{rom} u \quad (6)$$

where $q_{rom} = [x \ y \ z \ \phi \ \theta]^T$, f is the spring force, and $u_{2 \times 1}$ contains the torques of the leg angle and hip angle actuators mapped appropriately by B_{rom} . Taking $\xi = [q_{rom}^T \ \dot{q}_{rom}^T]^T$ as the state vector, one can write Eqn. 6 in the standard affine form:

$$\dot{\xi} = F(\xi, \xi) + G(\xi) u \quad (7)$$

where:

$$F = \begin{bmatrix} \dot{q}_{rom} \\ D_{rom}^{-1}(f - P) \end{bmatrix} \quad (8)$$

and:

$$G = \begin{bmatrix} 0 \\ D_{rom}^{-1} B_{rom} \end{bmatrix} \quad (9)$$

In this form, the input-output feedback linearization control law,

$$u = \left(\mathcal{L}_G \mathcal{L}_F \begin{bmatrix} \phi \\ \theta \end{bmatrix} \right)^{-1} \left(-K_1 \begin{bmatrix} \phi - \phi^d \\ \theta - \theta^d \end{bmatrix} - K_2 \begin{bmatrix} \dot{\phi} - \dot{\phi}^d \\ \dot{\theta} - \dot{\theta}^d \end{bmatrix} - \mathcal{L}_F^2 \begin{bmatrix} \phi \\ \theta \end{bmatrix} + \begin{bmatrix} \ddot{\phi}^d \\ \ddot{\theta}^d \end{bmatrix} \right) \quad (10)$$

wherein K_1 and K_2 are positive-definite matrices, leads to stable tracking of the desired variables. This completes the determination of the control inputs for all of the actuators of ATRIAS for stable in-place walking in three dimensions.

Walking with Nonzero Velocities

The controller proposed for in-place walking was based on regulating the horizontal plane impulse such that in the next step the projection of the velocity vector on the horizontal plane vanishes. To have a nonzero constant desired velocity, v^d , the discrete PID of Eqn. (5) is changed to:

$$\zeta_f = K_P (\zeta - v^d) + K_D (\zeta - \zeta_{n-1}) + K_I (\zeta - v^d t) + K_v \zeta \quad (11)$$

Although the above foot placement control can track small desired velocities ($< 0.5 - 0.6$ m/s), for larger velocities, due to the fact that energy loss increases with velocity, an energy injection scheme is necessary. Therefore, the neutral lengths of the springs are increased during stance (“push-off”) to have the corresponding actuators do positive work. Push-off can be done using different scenarios; but since the leg length force increases with push-off, it is desirable to start push-off after midstance to increase linear momentum as well. For the same purpose, one can remove energy in the first half of stance and then inject energy in the second half. Thereby, the linear momentum in the direction of the motion is always increased to overcome the resisting forces. In this regard, we propose δl_m , the additional term to be added to Eqns. (1) and (2) (depending on which leg is in stance phase), to be:

$$\delta l_m = \begin{cases} [k_{e1} v^d + k_{e2} (v^d - \dot{x})] \frac{x}{x_0} & x \leq 0 \\ [k_{e3} v^d + k_{e4} (v^d - \dot{x})] \frac{x}{x_0} & x > 0 \end{cases} \quad (12)$$

where k_{e1} , k_{e2} , k_{e3} , k_{e4} , and x_0 are nonnegative constants, and without loss of generality, x has been considered as the direction of motion.

States of the Legs

Traditionally, in the studies of dynamics and control of legged system, the touchdown is considered as a discrete switch between two distinct phases of locomotion. Formally, it means that the state of a leg belongs to one of the swing or stance sets. However, according to our experience, it is not simple to detect this switching point in practice, especially in fast, dynamic motions. Furthermore, this discrete switch demands that the states of the legs, before and after touchdown “match” each other (the very idea of HZD), which can become a limiting constraint.

In the present work, instead of looking at touchdown as a discrete switch, we utilize the mathematical concept of fuzzy sets to introduce a gradual shift between phases. In this way, the state of each leg is defined according to spring forces. Formally, stance phase of a leg is defined by a fuzzy set:

$$\mathcal{S}_t = \{(f, \mu_{st}(f)) | f \in F_l, \mu_{st}(f) \mapsto [0, 1]\} \quad (13)$$

where

$$\mu_{st}(f) = \begin{cases} 0 & f < \bar{f}_1 \\ \frac{f - \bar{f}_1}{\bar{f}_2 - \bar{f}_1} & \bar{f}_1 \leq f \leq \bar{f}_2 \\ 1 & f > \bar{f}_2 \end{cases} \quad (14)$$

in which f is the leg force, and \bar{f}_1 and \bar{f}_2 are predefined upper and lower limits. Similarly, the leg swing set is defined as:

$$\mathcal{S}_w = \{(f, \mu_{sw}(f)) | f \in F_l, \mu_{sw}(f) \mapsto [0, 1]\} \quad (15)$$

where $\mu_{sw}(f) = 1 - \mu_{st}(f)$. These fuzzy sets allow smooth transition between controls and phases, as it will be discussed in the next subsection.

Considerations for Implementation of the Controller on the Robot

For practical implementation on the robot, we need to translate all of the control logics presented in the previous sections to torques of the six actuators of the robot. The torques of the swing leg’s actuators can be obtained from PD controllers on motor position:

$$\tau_{sw} = \text{diag}(k_{P,m}) [q_m^d(l_m, \zeta_f) - q_m] + \text{diag}(k_{D,m}) [\dot{q}_m^d - \dot{q}_m] \quad (16)$$

where q_m is the vector of motor angles, and $k_{P,m}$ and $k_{D,m}$ are positive vectors. The vectors of desired motor angles and velocities are obtained from the kinematics of the mechanism.

Stance phase torques are obtained from l_m , δl_m , and u . Note that in ATRIAS the sagittal plane degrees of freedom are actuated with series elastic actuators, but the hip actuation is performed directly. Thus, if $u = [u_\phi \quad u_\theta]^T$, then:

$$\tau_{st} = \begin{bmatrix} u_\phi \\ k_{P,s} [q_{m,s}^d(l_m + \delta l_m, q_{rom}, u_\theta/k_s) - q_{m,s}] + k_{D,s} [\dot{q}_{m,s}^d - \dot{q}_{m,s}] \end{bmatrix} \quad (17)$$

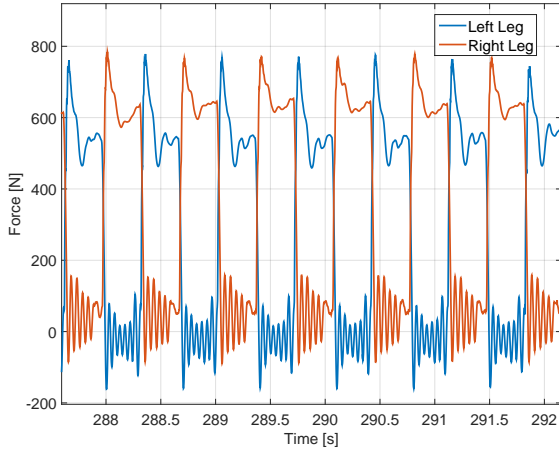


FIGURE 9: LEG FORCE IN AN INTERVAL OF A LONG STABLE IN-PLACE WALKING.

where $k_{P,s}$ and $k_{D,s}$ are sagittal plane motor proportional and derivative gains, k_s is the rotational spring stiffness, and $q_{m,s}$ represents the sagittal plane motor angles. For more detailed discussions on the kinematics of the mechanism see [26] and [29].

The commanded torque is obtained using the following standard defuzzification:

$$\tau = \mu_{sw} \tau_{sw} + \mu_{st} \tau_{st} \quad (18)$$

Note that $\mu_{sw} + \mu_{st} = 1$.

EXPERIMENTAL RESULTS

The controller proposed in the previous section was applied on ATRIAS for 3D in-place and forward walking. The robot is supported using a slack rope connected to a gantry in order to prevent it from falling and potential damages in unexpected conditions (Fig. 1).

Fig. 9 depicts the leg force in a part of long in-place walking test. The difference in the force profiles of the two legs is due to the fact that the center of mass of the torso is inclined to the right side, which demands the impulse of the right leg during one step to be larger. The controller has proven to be able to continue stable in-place walking for a long time and to have remarkable robustness against various types of disturbances, as can be seen in Fig. 10 and in [30], [31], and [32]. The controller has been also tested for a variety of walking tests. As an example, Fig. 11 depicts the desired and actual velocities during two different tests. The actual velocity has been estimated using proprioceptive data, assuming that always at least one leg is in stance and it is fixed on the ground. As can be seen in the figure, the controller can track any commanded (desired) velocity and unlike

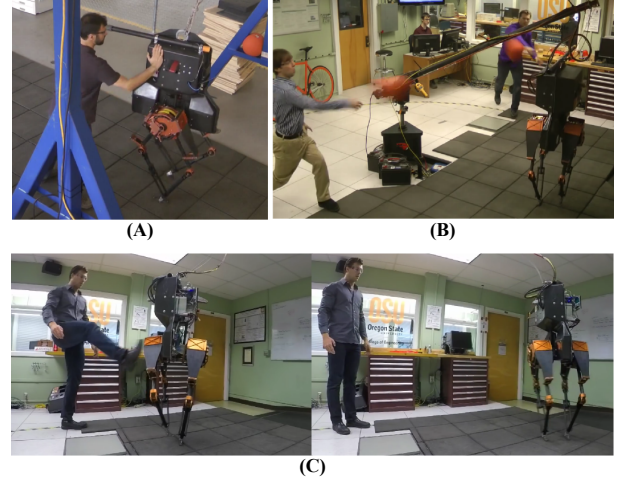


FIGURE 10: STILL IMAGES FROM VIDEOS OF ATRIAS MAINTAINING BALANCE WHILE BEING (A) PUSHED, (B) PELTED WITH DODGEBALLS AND (C) KICKED.

many other controllers proposed for such problems, is not limited to specific periodic orbits. The robot has been able to reach the speed of 4.3 kph (1.2 m/s) in a highly dynamic gait. To the authors' knowledge, in 3D, and especially with so many degrees of underactuation, this performance had not been shown by any other bipedal robot.

We have found that by tuning the controller gains, the tracking error can be significantly improved. Furthermore, due to limited length of our terrain (as can be seen in the video of this walking test [33]), testing higher velocities was not possible and we are aiming to resolve the problem by testing the robot in an outdoor environment and on a treadmill. The results of both these developments will be presented in the future publications.

The ground reaction forces of the last part of the experiment have been plotted in Fig. 12. Note that compared to in-place walking and due to energy injection, the forces become more and more similar to the standard “double-hump” spring-mass walking [24], which, in turn, qualitatively and quantitatively matches the human ground reaction force. In other words, with all complexities of ATRIAS compared to the original spring-mass template, the design methods and the invented control algorithms, have been faithful to our original philosophy of bipedal locomotion.

CONCLUSIONS

We presented a control framework based on the spring-mass model, and used it to control ATRIAS, a spring-mass robot, without planarizing constraints. This control resulted in robust stepping-in-place, capable of balancing in spite of pushes, kicks and dodgeball hits. Commanding non-zero velocity accelerated the robot to its new desired velocity, which reached a maximum

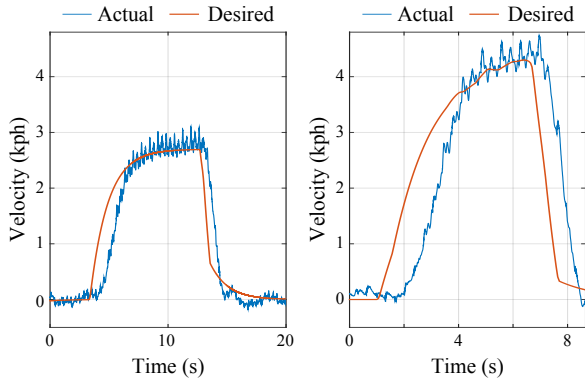


FIGURE 11: EXAMPLES OF EXPERIMENTS FOR VELOCITY TRACKING PERFORMANCE WITH DIFFERENT VELOCITIES (UP TO 4.3 KPH).

speed of 1.2 m/s (4.3 kph). Further, when plotting the ground-reaction forces of the resulting gait, they qualitatively match spring-mass model behavior, and consequently, the walking dynamics of humans. To our knowledge, this is the first reporting of human gait dynamics being replicated in a free-walking machine.

We argue that these results advance three overarching points. First, building controllers using simplified models is a promising means of generating a broader suite of behaviors for legged robots. With techniques such as hybrid zero dynamics, each gait is individually generated by an optimizer, and would have to be re-optimized for each desired speed. We demonstrate an alternate means for achieving gaits of varying speeds.

Second, unlike the underactuated control approaches suggested in the literature (such as HZD and transverse linearization) which typically use time-invariant methods, we have applied a time-based feedforward actuation to the system. This, as it was shown, has a strong (global) stabilizing effect, and is the key factor for the robustness and stability of the robot through exciting the compliant dynamics of it.

Lastly, it is important not to understate the interplay between the design of the robot’s passive dynamics and the method of control. As discussed before, the controller has been designed specifically using the reduced-order model(s) pertaining to dynamics of the robot. In other words, by understanding dynamics of the robot, although it is aggressively underactuated, the controller was able to make it walk in a robust, versatile, and biologically comparable fashion.

ACKNOWLEDGMENT

The authors acknowledge their funding support from the Defense Advanced Research Projects Agency (grant: W91CRB-11-1-0002), the Human Frontier Science Program (grant: RGY0062/2010), and the National science Foundation (grant:

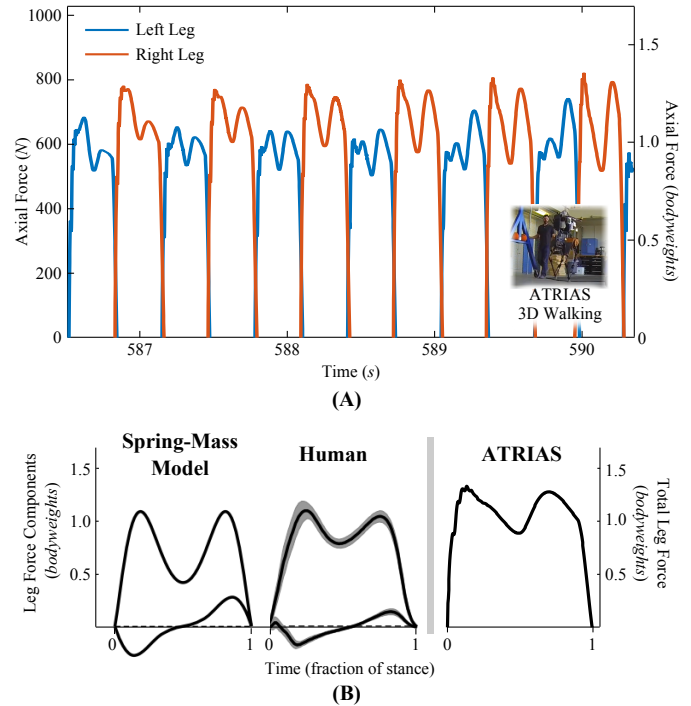


FIGURE 12: (A) AXIAL GROUND REACTION FORCES OF A 1.2 M/S (4.3 KPH) WALKING GAIT. THESE “DOUBLE-HUMPED” FORCES ARE CHARACTERISTIC OF SPRING-MASS WALKING, SHOWING THAT THE DYNAMICS OF THE SIMPLE MODEL ARE PRESERVED IN THIS COMPLEX MACHINE, AND (B) RESEMBLANCE OF WALKING FORCE PROFILES OF SPRING-MASS MODEL, ATRIAS, AND HUMANS [24] POINTS TO SIMILAR DYNAMIC CHARACTERISTICS.

CMMI-1100232).

REFERENCES

- [1] Spong, M., 1998. “Underactuated mechanical systems”. In *Control Problems in Robotics and Automation*, B. Siciliano and K. Valavanis, eds., Vol. 230 of *Lecture Notes in Control and Information Sciences*. Springer Berlin / Heidelberg, pp. 135–150.
- [2] Raibert, M. H. H., 1986. *Legged robots that balance*, Vol. 29. MIT Press, Mass.
- [3] Sakagami, Y., Watanabe, R., Aoyama, C., Matsunaga, S., Higaki, N., and Fujimura, K., 2002. “The intelligent ASIMO: system overview and integration”. pp. 2478–2483.
- [4] Vukobratovic, M., and Juricic, D., 1969. “Contribution to the synthesis of biped gait”. *Biomedical Engineering, IEEE Transactions on*(1), pp. 2–7.
- [5] Stephens, B. J., and Atkeson, C. G., 2010. “Dynamic Balance Force Control for compliant humanoid robots”. 2010

- IEEE/RSJ International Conference on Intelligent Robots and Systems*, Oct., pp. 1248–1255.
- [6] Pratt, J., Koolen, T., de Boer, T., Rebula, J., Cotton, S., Carff, J., Johnson, M., and Neuhaus, P., 2012. “Capturability-based analysis and control of legged locomotion, Part 2: Application to M2V2, a lower-body humanoid”. *The International Journal of Robotics Research*, **31**(10), Aug., pp. 1117–1133.
- [7] Stephens, B. J., and Atkeson, C. G., 2010. “Push Recovery by stepping for humanoid robots with force controlled joints”. *2010 10th IEEE-RAS International Conference on Humanoid Robots*, Dec., pp. 52–59.
- [8] McGeer, T., 1990. “Passive dynamic walking”. *International Journal of Robotics Research*, **9**(2), pp. 62–82.
- [9] Spong, M. W., 1994. “Partial Feedback Linearization of Underactuated Mechanical Systems”. In *IEEE/RSJ Intl. Conf. on Intelligent Robots and Systems*, pp. 314–321.
- [10] Collins, S. H., Ruina, A., Tedrake, R., and Wisse, M., 2005. “Efficient Bipedal Robots Based on Passive Dynamic Walkers”. *Science Magazine*, **307**(5712), pp. 1082–1085.
- [11] Bhounsule, P. A., Cortell, J., Grewal, A., Hendriksen, B., Karssen, J. D., Paul, C., and Ruina, A., 2014. “Low-bandwidth reflex-based control for lower power walking: 65 km on a single battery charge”. *The International Journal of Robotics Research*, **33**(10), pp. 1305–1321.
- [12] Westervelt, E. R., Grizzle, J. W. W., and Koditschek, D. E. E., 2003. “Hybrid Zero Dynamics of Planar Biped Walkers”. *IEEE Transactions on Automatic Control*, **48**(1), Jan., pp. 42–56.
- [13] Park, H., Sreenath, K., Ramezani, A., and Grizzle, J. W., 2012. “Switching control design for accommodating large step-down disturbances in bipedal robot walking”. In *IEEE/RSJ International Conference on Robotics and Automation (ICRA)*, Ieee, pp. 45–50.
- [14] Yadukumar, S. N., Pasupuleti, M., and Ames, A. D., 2012. “Human-Inspired Underactuated Bipedal Robotic Walking with AMBER on Flat-ground, Up-slope and Uneven Terrain”. In *IEEE/RSJ International Conference on Intelligent Robots and Systems (IROS)*.
- [15] Sreenath, K., Park, H.-W., Poulakakis, I., and Grizzle, J., 2013. “Embedding active force control within the compliant hybrid zero dynamics to achieve stable, fast running on MABEL”. *The International Journal of Robotics Research*, **32**(3), Mar., pp. 324–345.
- [16] Sinnet, R. W., and Ames, A. D., 2012. “Extending Two-Dimensional Human-Inspired Bipedal Robotic Walking to Three Dimensions through Geometric Reduction”. In *2012 American Control Conference*.
- [17] Buss, B. G., Ramezani, A., Akbari Hamed, K., Griffin, B. A., Galloway, K. S., and Grizzle, J. W., 2014. “Preliminary Walking Experiments with Underactuated 3D Bipedal Robot MARLO”. In *Intelligent Robots and Systems (IROS 2014)*, IEEE, pp. 2529–2536.
- [18] Manchester, I. R., Mettin, U., Iida, F., and Tedrake, R., 2011. “Stable dynamic walking over uneven terrain”. *The International Journal of Robotics Research*, **30**(3), Jan., pp. 265–279.
- [19] Erez, T., Lowrey, K., Tassa, Y., and Kumar, V., 2013. “An integrated system for real-time Model Predictive Control of humanoid robots”. In *IEEE/RAS International Conference on Humanoid Robots*.
- [20] Blickhan, R., 1989. “The Spring-Mass Model for Running and Hopping”. *J. of Biomech.*, **22**(11/12), pp. 1217–1227.
- [21] Holmes, P., Full, R. J. R. J., Koditschek, D. E. D., and Guckenheimer, J., 2006. “The Dynamics of Legged Locomotion: Models, Analyses, and Challenges”. *SIAM Review*, **48**(2), May, pp. 207–304.
- [22] Andrews, B., Miller, B., Schmitt, J., and Clark, J. E., 2011. “Running over unknown rough terrain with a one-legged planar robot.”. *Bioinspiration & biomimetics*, **6**(2), June, p. 026009.
- [23] Wu, A., and Geyer, H., 2013. “The 3-D Spring-Mass Model Reveals a Time-Based Deadbeat Control for Highly Robust Running and Steering in Uncertain Environments”. *IEEE Transactions on Robotics*, **29**(5), Oct., pp. 1114–1124.
- [24] Geyer, H., Seyfarth, A., and Blickhan, R., 2006. “Compliant leg behaviour explains basic dynamics of walking and running”. *Proc. R. Soc. Lond. B.*, **273**(1603), Nov., pp. 2861–2867.
- [25] Hubicki, C., Grimes, J., Jones, M., Renjewski, D., Sprowitz, A., Abate, A., and Hurst, J., 2015. “ATRIAS: Enabling Agile Bipedal Locomotion with a 3D-Capable Spring-Mass Robot Design”. In *Submission*.
- [26] Rezazadeh, S., and Hurst, J. W., 2015. “Toward Step-by-Step Synthesis of Stable Gaits for Underactuated Compliant Legged Robots”. In *accepted for The 2015 IEEE International Conference on Robotics and Automation (ICRA)*.
- [27] Koditschek, D. E., and Buhler, M., 1991. “Analysis of a Simplified Hopping Robot”. *The International Journal of Robotics Research*, **10**(6), Dec., pp. 587–605.
- [28] Schmitt, J., and Clark, J., 2009. “Modeling posture-dependent leg actuation in sagittal plane locomotion.”. *Bioinspiration & biomimetics*, **4**(4), Dec., p. 046005.
- [29] Ramezani, A., Hurst, J. W., Akbari Hamed, K., and Grizzle, J. W., 2013. “Performance Analysis and Feedback Control of ATRIAS, A Three-Dimensional Bipedal Robot”. *Journal of Dynamic Systems, Measurement, and Control*, **136**(2), Dec., p. 021012.
- [30] <https://youtu.be/yYvrTc3-uVU>.
- [31] <https://youtu.be/5BF3uzXWfDY>.
- [32] <https://youtu.be/7b53L10RaIE>.
- [33] <https://youtu.be/5Y5aQqhjE7U>.